Supplementary Materials

Table of Contents

1. Kinetics Equations for the Photo-bleaching 2
2. Chromeo546 and RFP-mCherry 4
3. Finite Element Simulation 4
4. Thiol-tagged DNA 6
5. Reference: 6

1. Kinetics Equations for the Photo-bleaching

To help better understand the photo-bleaching limit and the dynamic process of fluorescence, we employ a simplified two level systems shown in the right panel in the figure below. A ground stated fluorophore, denoted as *g*, could be excited to an excited state *e*, at a rate of $k_A g$. The excited fluorophore *e* then relaxes back to the ground state *g*, either though fluorescence k_f by emitting a photon, or a non-radiative channel k_{iNR}, where the energy is dissipated as heat. The excited fluorophore *e* could also undergo a chemical reaction and lose its fluorescence capability permanently at a photo-bleaching rate with a rate constant of Γ. Thus we can use a set of kinetics equations to model the excitation, the relaxation and the bleaching process as follows:

$$\begin{aligned} \frac{d}{dt}e &= -\left(k_f + k_{iNR} + \Gamma\right)e + k_A g \\ \frac{d}{dt}g &= \left(k_f + k_{iNR}\right)e - k_A g \end{aligned} \qquad (1)$$

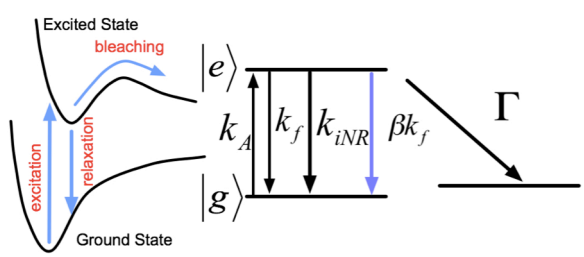

S1 A Kinetics Model.

From Eq. (1) we can calculate the average lifespan of a fluorophore, the time that a fluorophore continuously emitting photons before being bleached:

$$\int_0^\infty te(t)dt \Big/ \int_0^\infty e(t)dt = \left(k_f + k_{iNR} + k_A + \Gamma\right)/\Gamma k_A \qquad (2)$$

We use the term lifespan here to distinguish it from another term, lifetime, which is the time it takes for an excited fluorophore to relax back to its ground state, defined as $1/(k_{iNR}+k_f)$. For most fluorophore, the relaxation process k_{iNR}, and k_f are on the order of $1ns^{-1}$, which is much bigger than the bleaching rate constant Γ and the excitation rate constant k_A, both of which are around 1 ms^{-1}, thus the average lifespan is $\tau \approx k_f/\Gamma q k_A$, where *q* is the fluorescence quantum yield of the fluorophore defined as $q=k_f/(k_f+k_{iNR})$.

Since the observed fluorescence (spontaneous emission) intensity is $k_f e$, integrating it over time, we arrive at a simple result, the total number of photons that a fluorophore can emit before it bleaches, the photo-bleaching limit, is:

$$\text{Photo-Bleaching Limit} = \int dt k_f e(t) = k_f/\Gamma \qquad (3)$$

Because $k_A=C_{abs}|E|^2$, where E is the local electromagnetic field, and C_{abs} is the molecular absorption cross-section, the lifespan is inversely proportional to the local field as $\tau \propto 1/|E|^2$, and the photo-bleaching limit is *independent* of the local field.

The kinetics equation can also calculate the quantum yield of the photo bleaching(*1*)—the probability of a reaction after absorbing one photon:

$$\Phi = \Gamma/\left(k_f + k_{iNR} + \Gamma\right) \approx q\Gamma/k_f \qquad (4)$$

Here q is the fluorescence quantum yield.

Equations (2) and (5) show that increasing the fluorescence rate k_f can suppress the photo bleaching as effectively as reduction of the bleaching rate constant Γ.

Suppose we can enhance the spontaneous-emission of a molecule by a factor of β. Substituting it into the kinetics equations show that the lifespan of the molecule will be increased to,

$$\tau = k_f(\beta+1/q-1)/\Gamma k_A \qquad (5)$$

and the total number of photons that the molecule can emit is,

$$\beta\eta k_f/\Gamma \qquad (6)$$

Here q is the fluorescence quantum yield, defined as $q=k_f/k_f+k_{iNR}$, of the molecule, and η is an efficiency factor brought in to account for extra non-radiative channels introduced as a byproduct of the β. The calculation of these two factors, β and η will be exemplified in detail later. For a practical application, both high β and η are important for practical applications.

We can also calculate the new quantum yield of the photo bleaching as:

$$\Phi = \Gamma/\left(\beta k_f + k_{iNR} + \Gamma\right) \approx q\Gamma/k_f(\beta q - q + 1) \qquad (7)$$

Because a commonly used fluorescent molecule usually exhibits high quantum yield, q~1, and both Γ and k_A of the molecule are much smaller than the relaxation constants k_f and k_{iNR}, with Γ and k_A around ms^{-1}, and k_f and k_{iNR} around ns^{-1}(*2-4*), we can simplify the results by neglecting these factors. Hence, comparing Eqs (5-7) with Eqs (2-4), we can see that the lifespan and the total number of photon emitted can increase by β and $\beta\eta$ times respectively, and the bleaching quantum yield reduce by about β times.

For weak fluorescent dyes, whose fluorescence quantum yield q<<1, the improvement of the total number of photons is the same as $\beta\eta$ times. However, the improvement of the lifespan τ and the bleaching quantum yield Φ is about $q\beta$ times. This is because the enhanced vacuum fluctuation only affects the spontaneous emission of a molecule, which is, q fraction of the total relaxation process of the molecule.

Because plasmonic nano structures can have high Purcell factor β>1,000, suppression of photo bleaching should be observed even for weak dye whose fluorescence quantum yield q is larger than $1/\beta$~0.001.

2. Chromeo546 and RFP-mCherry

To confirm the generality of our approach, we repeat an identical single molecule experiments on a different small molecule dye, chromeo546 whose emission centers at 561nm. A 532nm laser is used as the excitation source. The result is shown in Fig. S2, the same antenna structure exhibits similar suppression of the photobleaching.

The approach isn't limited to small molecules, but also can be applied to large

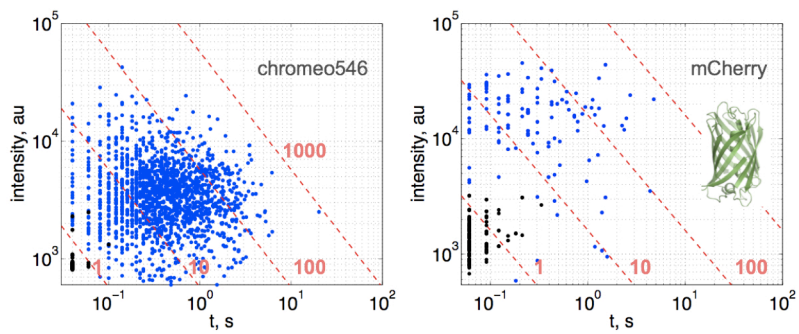

S2 Chromeo 546 and mChery

biological molecules. Fig. S2 exhibits the experiment results on red fluorescent protein mCherry. We observe similar giant photobleaching suppression.

3. Finite Element Simulation

We perform numerical simulations using a commercial finite-element solver (COMSOL Multiphysics), on a simple nano antenna consisting of two gold nanoparticles

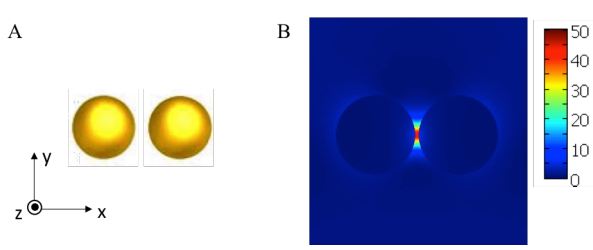

S3 A Nano Antenna (A) Schematic of the optical antenna consisting of two gold nanoparticles. (B) Electric field enhancement when plane wave is incident along y-axis and polarized along x-axis.

depicted in the figure below. The diameter of the gold sphere is 100 nm, and the gap between the spheres is 5 nm. At 660 nm wavelength, The permittivity of gold is ε_m=-13.6+1.035i(*5*) . First, a plane wave excitation is applied with the propagation along the

y-axis and polarization along the x-axis. Under this condition, the fundamental dipole modes of the two gold spheres are excited. The electric field within the tiny gap is dramatically enhanced up to 48.7 (Panel B), corresponding to an intensity enhancement about 2500. Away from the gap, the field intensity quickly drops as shown in Fig. 3(A) in the main text.

We then model a fluorophore as a dipole at different polar positions. When the dipole radiation matches the mode profile of the dipole antenna, i.e. orients along the x-axis, its oscillation will be enhanced significantly. The radiative power is obtained by integrating the Poynting vector over a surface that encloses the dipole and the gold nano particles. The non-radiative power due to the metal Ohm loss is calculated by the volume integration of *jxE* for the two gold spheres. Compared with the dipole radiation in free space without the optical antenna, the maximum enhancement factors of radiative emission and non-radiative emission are 2800 and 1400, respectively, when the fluorophore is centered at the gap region (red line in figure S5, panel B and C). More importantly, the radiative emission efficiency is still as large as 65.7% (Panel D), indicating the optical antenna performs very efficiently.

For comparison, we also simulate dipole oriented along the y-axis and z-axis,

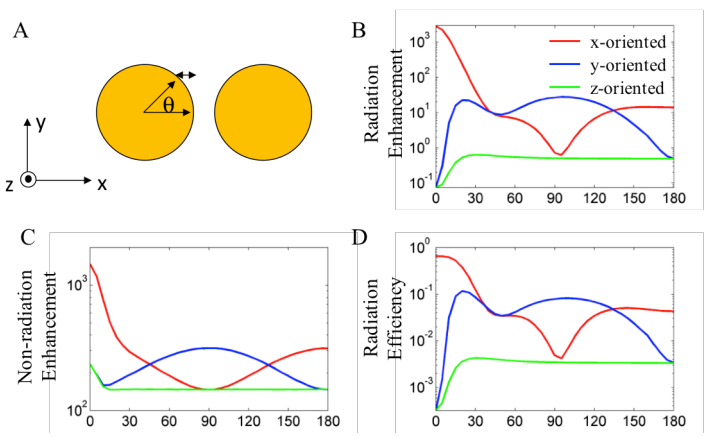

S4 (A) Schematic of simulation process. A dipole source with different orientations is placed 2.5nm away from the particle at different polar angles. (B) Radiation enhancement, (C) Non-radiation enhancement and (C) Radiation efficiency η for three dipole orientations.

which are plotted in blue and green lines respectively in panel (B)-(D) of the figure S4. One can see that the radiation enhancement is fairly low, especially for dipoles orientated in z direction, which suggests that optical antenna is hardly excited.

In addition to the dimer, we have simulated the timer consisting of three gold nano particles as shown in next figure. The field enhancement is about 47 when the gaps between particles are 5 nm, comparable with that of the dimer. Following the same procedure, we have calculated the maximum radiative emission enhancement,

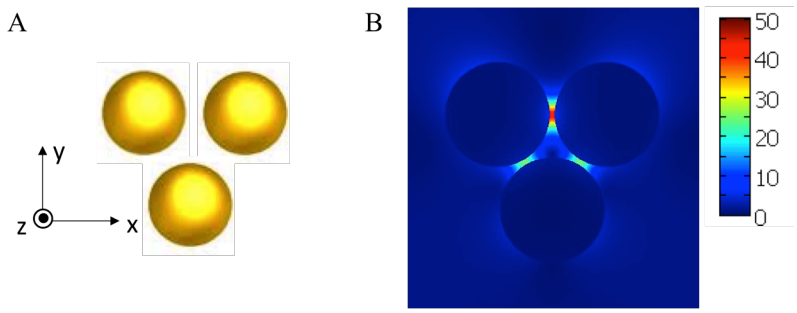

S5 (A) Schematic of a trimer consisting of three gold nanoparticles. (B) Electric field enhancement when plane wave is incident along y-axis and polarized along x-axis.

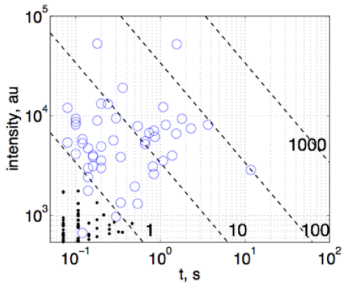

S6 thiol-drivated ssDNA-Cy5. The blue circles are data from gold nano clusters, the black dots are from the surface of quartz slides.

non-radiative emission enhancement and radiative emission efficiency, which are 2408, 1645 and 59.5%, respectively. This result further confirms our experimental approach and observation.

4. Thiol-tagged DNA

Thiol-derivatized DNA molecules interact strongly with the gold surface through the sulfur atom of the thiol group. This interaction has been utilized extensively for self-assembly of metallic nanostructures. We also conducted experiments with thiol-derivated DNA tagged with Cy5 dye /5Cy5/GGA GGA AGC TTG GAG GCA GTC GGA AAT AAC/3ThioMC3-D/ (from IDT). We have observed similar results (Fig. S6).

5. Reference:

1. N. J. Turro, *Journal of Chemical Education* **44**, 536 (1967).
2. J. R. Lakowicz, *Principles of Fluorescence Spectroscopy*. (Springer, New York, ed. 3, 2006).
3. N. J. Turro, *Modern Molecular Photochemistry*. (University Science Books, 1991), pp. 628.
4. L. Song, E. J. Hennink, I. T. Young, H. J. Tanke, *Biophysical Journal* **68**, (1995).
5. P. B. Johnson, R. W. Christy, *Physical Review B* **6**, 4370 (1972).